This paper is a pre-print version of:
Cipolla, V., Frediani, A., Lonigro, E. *et al.* Aerodynamic design of a light amphibious PrandtlPlane: wind tunnel tests and CFD validation. *Aerotec. Missili Spaz.* **94,** 113–123 (2015). https://doi.org/10.1007/BF03404694

Aerodynamic design of a light amphibious PrandtlPlane: wind tunnel tests and CFD validation

A. Frediani[1], V. Cipolla[2], E. Lonigro[3], F. Oliviero[4],
University of Pisa, 56122 Pisa, Italy

Wind tunnel tests have been carried out on a ¼ scaled model of a two seats amphibian PrandtlPlane. In the present paper, CFD analyses, conducted with the Star-CCM+ software in order to replicate the experimental results, are presented. First, the full-scale free-air conditions have been simulated with a k-ε model and the results compared with those for the ¼ scaled model; the effects of the different Reynolds numbers are discussed. Then, by adding the elements connecting the model to the wind tunnel, i.e. the pylon and the walls, new simulations have been carried out with significant effects in the case of some aerodynamic derivatives. Finally, in order to improve the agreement between experimental and CFD results, further studies have been conducted with a fixed transition k-ω turbulence model. The results of the CFD analyses are exposed and discussed, the advantages and the disadvantages of k-ε and k-ω models are compared and general conclusions are given on the role of CFD and wind tunnel in the aerodynamic design of a modern aircraft and, more in particular, of the amphibian PrandtlPlane at hand.

Nomenclature

α = angle of attack [°]

β = angle of sideslip [°]

CL = Lift coefficient

CD = Drag coefficient

CY = Side force coefficient

Cm = Pitch moment coefficient

[1] Full Professor, Department of Civil and Industrial Engineering (Aerospace Section). Via Caruso 8, 56122 Pisa, (Italy). E-mail: a.frediani@dia.unipi.it.
[2] Postdoctoral Research Fellow, Department of Civil and Industrial Engineering (Aerospace Section). Via Caruso 8, 56122 Pisa (Italy). E-mail: v.cipolla@for.unipi.it.
[3] M.Sc. Degree in Aerospace engineering. University of Pisa.
E-mail: lonigro.eugenio@gmail.com
[4] PhD Student, Department of Civil and Industrial Engineering (Aerospace Section). Via Caruso 8, 56122 Pisa (Italy). E-mail: f.oliviero@for.unipi.it.

This paper is a pre-print version of:
Cipolla, V., Frediani, A., Lonigro, E. *et al.* Aerodynamic design of a light amphibious PrandtlPlane: wind tunnel tests and CFD validation. *Aerotec. Missili Spaz.* **94,** 113–123 (2015). https://doi.org/10.1007/BF03404694

Cl = Roll moment coefficient

Cn = Yaw moment coefficient

1. INTRODUCTION

The present paper is a part of a two-year research project called IDINTOS, coordinated by the Aerospace Section of DICI (Department of Civil and Industrial Engineering), Pisa University and co-founded by the Regional Government of Tuscany (Italy). The final goal of the project was the design and the construction of a full-scale prototype of an innovative two seats amphibious PrandtlPlane; the research project included also wind tunnel, towing tank and scaled model flight tests. The project was concluded with the manufacturing of the prototype; Fig. 1 shows the presentation in Friedrichshafen 2014 and Fig. 2 shows the cockpit of the same aircraft. More details on the IDINTOS project can be found in [1] and [2].

Fig. 1 IDINTOS presentation at AERO2014 (Friedrichshafen, Germany)

Fig. 2 The cockpit of IDINTOS

The name PrandtlPlane indicates an aircraft configuration in honor of L. Prandtl. According to Prandtl there exist a configuration which provides the minimum induced drag for given lift and wingspan; this configuration, called "best

wing system" (BWS), is a proper box-wing (Ref. [3]), in which the conditions given by Munk theorems are satisfied. Many engineering applications on aircraft design of the Prandtl's BWS concept are possible, as shown in [4]; in the case at hand the application is relevant to a light two seats aircraft; in this case the advantages on the induced drag reduction are not fully exploited compared to the very large aircraft, but other advantages are available as far as safety of flight is concerned. Both CFD and wind tunnel data show that the PrandtlPlane lifting system has great stability at stall and a very smooth behavior in post-stall conditions, thanks to the rear wing which provides a significant lift even when front wing is stalled. Flight safety is even more increased in terms of maneuverability by means of counter-rotating elevators placed on both front and rear root wings, which introduce a pure moment instead of a vertical tail force, allowing a more precise and safer pitch control.

The amphibian object of the present study is characterized by a box-wing lifting system, retractable landing gears, floating fuselage, two wingtip auxiliary floats and one thermal engine, positioned into the fuselage, which drives two ducted propellers by belts (the ducts are currently under construction and are not shown in the pictures). Technical data are listed in Table 1.

Table 1 Main data of the IDINTOS full-scale prototype

Wingspan	8 m
Wing Area (front+rear)	14.1 m^2
Max. Take-Off Weight	650 kg
Seats	2 side-by-side
Engine Power	100 Hp
Max level flight speed (h=1000m, estimated)	69 m/s
Stall speed w. full flaps (sea level, estimated)	21 m/s

As said before, towing tank tests have been performed during the project at CNR-INSEAN facilities in Rome on a ⅓ scaled model of the hull (Fig. 3) and wind tunnel tests have been carried out at Milan Politecnico wind tunnel on a ¼ scaled model (Fig. 4**)**. Details on such activities can be found in [5] and [6], respectively.

Wind tunnel tests have been followed by the construction of a ¼ scaled flying model with two electric engines with conventional propellers mounted as the ones of the full-scale prototype, shown in Fig. 5; the flying model had its first take-off in July of 2014, collecting a huge amount of data related to various flight conditions.

This paper is a pre-print version of:
Cipolla, V., Frediani, A., Lonigro, E. *et al.* Aerodynamic design of a light amphibious PrandtlPlane: wind tunnel tests and CFD validation. *Aerotec. Missili Spaz.* **94,** 113–123 (2015). https://doi.org/10.1007/BF03404694

Fig. 3 Towing tank tests on the 1⅓ scaled model of the hull at CNR-INSEAN in Rome

Fig. 4 Wind tunnel tests on IDINTOS ¼ scaled model

Fig. 5 Flight tests on the IDINTOS scaled model.

All the aerodynamic derivatives regarding the aircraft have been obtained both with CFD simulations and wind tunnel tests; examples are the derivatives regarding the single controls (front and rear ailerons, front and rear elevators, front (it is a fowler) and rear (plain) flaps; besides, the derivatives have been determined with the twin controls acting at the same time, in order to verify whether the superposition of effects is applicable in this complex aircraft configuration and, eventually, in what ranges. In general, it can be said that the CFD results (in the condition of open air) and the experimental ones (in the wind tunnel) correspond very closely in the linear range for the angles of attack and yaw and, in the case of the controls, in the initial range of the actuation angles. The results here presented have the limited objective of analyzing some particular cases in which nonlinearities found from wind tunnel tests have not been reproduced properly by the CFD analysis. More results of wind tunnel tests can be found in [6].

2. WIND TUNNEL TESTS AND CFD ANALYSIS

The wind tunnel tests have been carried out at the wind tunnel facility of the Politecnico di Milano (Italy), whose characteristics are shown in Table 2, on a ¼ scaled model of the amphibian, provided with elevators, fowler flaps on front wing, plain flaps on rear wing, ailerons and rudder (Fig. 6). The model is made of polyurethane-based resin, reinforced with aluminum ribs and steel spars[5] inside.

Fig. 6 Details of the IDINTOS wind tunnel test model

[5] The model has been built at the Department of Civil and Industrial Engineering, with the collaboration of EDI Progetti S.r.l.

Table 2 Characteristics of the wind tunnel facility of Milan Politecnico

Type of circuit	Closed
Test section shape	Square
Test section dimensions	W=4m, H=3.84m, L=6m
Maximum speed	55m/s
Turbulence level	< 0.1%

The main goal of the wind tunnel tests was to verify the fulfillment of requirements (Ref. [7]) on sport aircraft, for both cruise and landing/take-off conditions. The results here summarized are further explained in [6]. Using a closed, squared test section several conditions on both longitudinal and lateral-directional planes were studied, collecting data with a 6-components balance.

The wind speed of the tunnel was 40 m/s when simulating cruise conditions and 30 m/s in the flapped configurations; correspondingly, the Reynolds numbers are $6.3 \cdot 10^5$ and $4.7 \cdot 10^5$, corresponding to 18% and the 42% of the full-scale Reynolds numbers, respectively. Finally, the model has been mounted on a strut (Fig. 7), acting as a support for the balance and providing pitch and yaw rotations to the model.

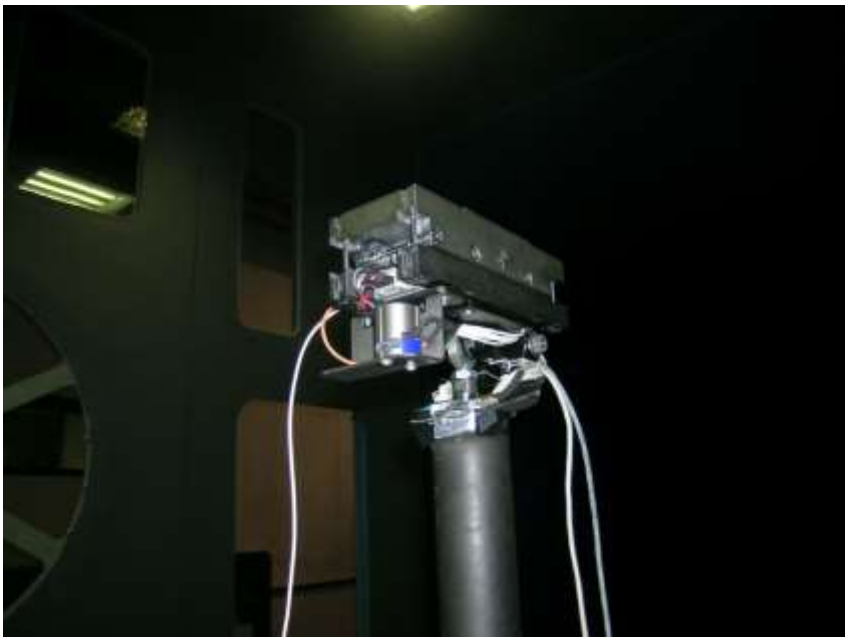

Fig. 7 The 6-components balance and the strut

In order to simulate the wind tunnel conditions in the CFD analysis, the CAD model of the full-scale aircraft was first reduced by a ¼ factor; then, the pylon and, finally, the tunnel walls were added to the model, as shown in Fig. 8.

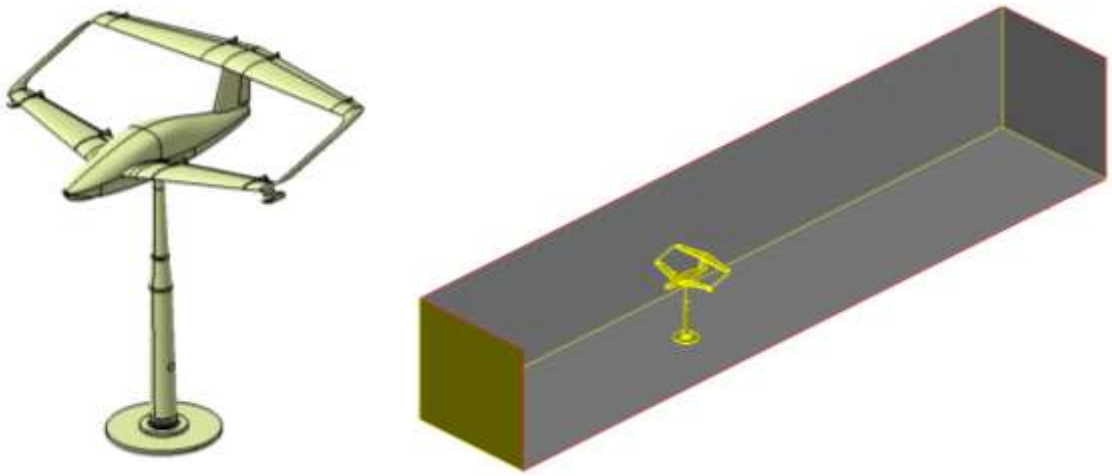

Fig. 8 Pylon and pylon plus walls.

The surface mesh used for the IDINTOS model is the result of a preliminary analysis on the mesh sensibility; then, surface meshes for the pylon and the tunnel walls were added and, thus, the fluid region of the CFD analysis was defined. A volume mesh was generated inside, by the Star-CCM+ algorithm, providing the appropriate refinement in the wake region and nearby the airplane surface.

The resulting mesh is polyhedrical and, in particular, prismatic along the walls; in total it is composed of about 32 million elements. To compare the CFD with the wind tunnel results, several values of α (pitch) and β (yaw) angles were considered, covering the ranges $\alpha = -5° \div 12°$ and $\beta = 0° \div 10°$. The analysis is made of two parts; the first one was conducted with a fully turbulent k-ε model and, in the second one, a k-ω turbulence model with fixed transition was introduced.

2.1 Transition settings

The boundary layer transition must be assessed with a simple and fast method and, in this context, we have adopted here a method based on a simple visualization, in the framework of linear analysis of perturbations (since the surface is smooth and hypothesis of small perturbations is valid). First, a $pseudo - Re = \frac{\rho(P)*U(P)*L(P)}{\mu}$ field function has been defined; this function assumes a certain value in any point of the fluid region, due to the combination of the local values of density, velocity and local length. The pseudo-Re are assessed in the points located on the border of the boundary layer, where, according to the boundary layer linear stability theory, the transition occurs when the local Reynolds number equals a certain critical value. According to this theory, the points on the boundary layer with pseudo-Re value = $5*10^5$ are determined and the set of these points define the lines of transition; an example is shown in Figure 10, based on the results obtained by Star-CCM+ software.

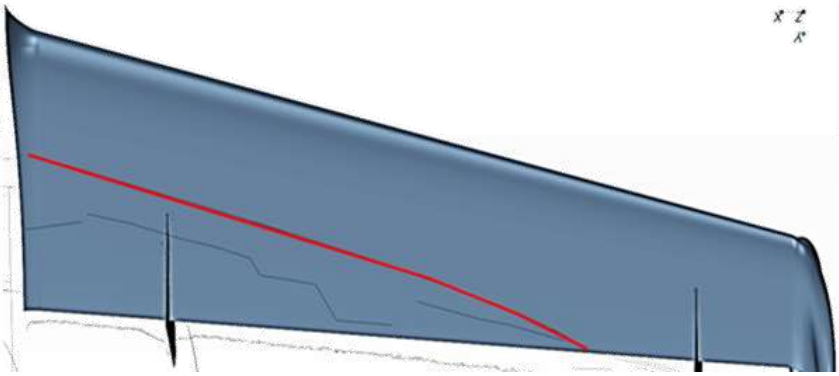

Fig. 9 Transition line on the upper surface of the front wing for α=1 °

The method is applied to the wings and, in practice, it is implemented as follows. First, a local coordinate system is generated, so that the x=0 coordinate is placed in front of the trailing edge of the surface studied and the x axis is directed normally to the edge itself; then, a surface with the same Reynolds of 500.000 inside the fluid region is generated, whose a typical section is shown in Figure 11.

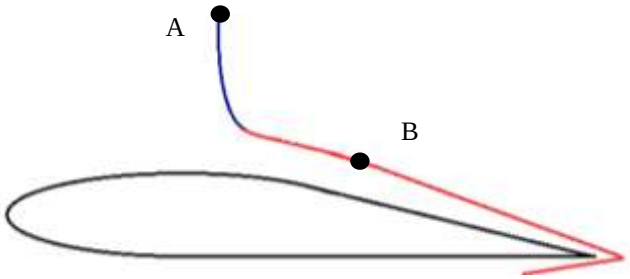

Fig. 10 Pseudo-Re isosurface.

Sectioning the isosurface one can notice that at some point the surface bends to a quasi-horizontal position. This is an effect of the entrance in the boundary layer. In fact, moving downside the surface from A to B, speed drastically decreases and to achieve the critical pseudo-Re value the isosurface starts to move to valley, where the local length value is higher. So, it is hence assumed that the points on the border of the boundary layer are located where the isosurface bends more strongly, which is in Fig. 10 the point where the isosurface color turns from blue to red. Finally, visualizations as in Fig. 9 are obtained just highlighting the points of the surface with the strongest curvature.

This method is based on some arbitrary assumptions, as the critical value of Reynolds and, also, the location of the transition is affected by errors. However, we have the possibility of validating the method on the basis of the wind tunnel results and the conclusion is that, as shown later on, the maximum error observed in the comparison between the CFD results and experimental data for CL and CD is not higher than 3 - 4%; besides, the method has no practical computational cost because we use existing tools in the aerodynamic code.

This paper is a pre-print version of:
Cipolla, V., Frediani, A., Lonigro, E. *et al.* Aerodynamic design of a light amphibious PrandtlPlane: wind tunnel tests and CFD validation. *Aerotec. Missili Spaz.* **94,** 113–123 (2015). https://doi.org/10.1007/BF03404694

Once the k-ω simulation have been established, the final CFD work plan of the CFD computations is reported in Table 3.

Table 3 Wind tunnel CFD simulations work plan

CFD Model	Scale	Geometry	Solver	α [°]	β [°]
1	1:1	Airplane	k-ε	1	0 – 12
2	1:4	Airplane	k-ε	1	0 – 12
3	1:4	Airplane + Pylon	k-ε	1 - 12	0
4	1:4	Airplane + Pylon + Tunnel walls	k-ε	1 - 12	0 – 12
5	1:4	Airplane + Pylon + Tunnel walls	k-ω fixed transition	1 - 12	0 – 12

3. WIND TUNNEL RESULTS

The wind tunnel results shown in the following section are related to the clean configuration, i.e. with undeployed flaps.

The CL and CM vs α, summarized in Fig. 11, show that a smooth stall begins for an angle of attack of about 17°; the Cmα derivative is negative in the whole range of angle of attack (and, hence, the aircraft is stable), with two quasi-linear ranges (when a first stall occurs, the front wing stalls first and the rear one produces a more negative pitching moment)

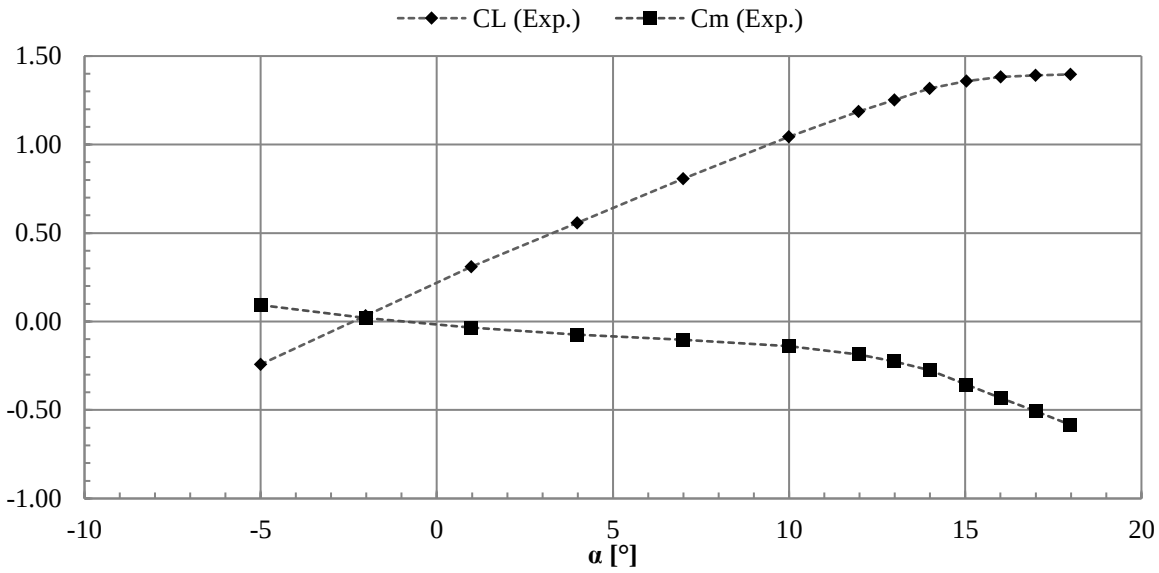

Fig. 11 Experimental CL-α and Cm-α curves.

The wind tunnel results are not so clear in the presence of yaw; with reference to Figure 13, the most unexpected results concern the behavior of the yaw moment (Cn) vs yaw angle (β) at different angles of attach. At 1° of incidence, the derivative Cn_β is negative (and the aircraft is stable in the lateral plane) in the whole range of yaw angles, with the

exception of the intermediate range 6°-8°. This situation is totally different at high angles of attack (α=12°), where the lateral stability appears to be small or nil for small β values and is higher at higher yaw angles (>6°).

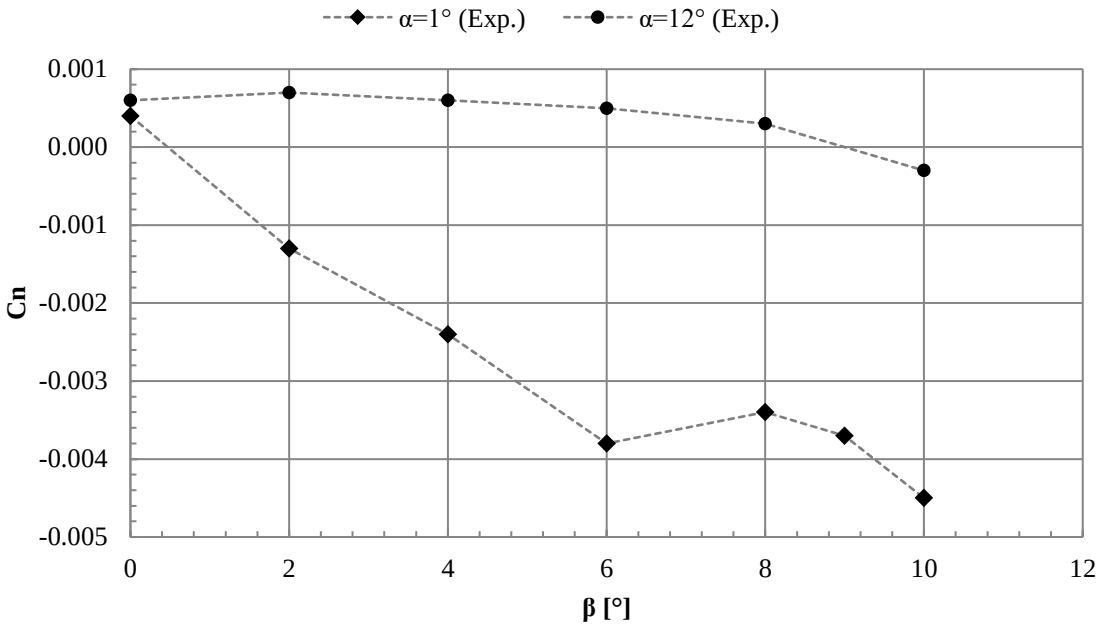

Fig. 12 Experimental Cn-β curves at α=1° and α=12°

All the other derivatives involving lift (Cl) and lateral force (CY) coefficients are linear all over the whole β range and, correspondingly, CFD and wind tunnel experimental results are coincident. Thus, the only CFD analysis presented here in the case of yaw derivatives is limited to study the cases in Figure 13; in particular, we wish to give an explanation (if any) to the lateral instability occurring in the range 6° - 8° of β because it regards the safety of the aircraft; another problem is, from figure 13, the lack of lateral stability at low incidence (α=1°) in the case of moderate angles of yaw (β = 0° - 6°).

4. CFD ANALYSIS AND VALIDATION THROUGH WIND TUNNEL DATA.

The CFD analysis was carried out in different steps. According to Table 3, the first one is a simulation of the full-scale aircraft in free air and cruise conditions with the k-ε vorticity (CFD model 1); since the results were not close to those from the wind tunnel tests, the model was scaled to ¼ dimensions (CFD model 2); then, the pylon was added, still

in the condition of free air (CFD model 3); afterwards, the tunnel walls were introduced into CFD model 3 to enclose the fluid region (CFD model 4); finally, the k-ω transition model was introduced into CFD model 4 (CFD Model 5).

The results have been divided in two parts, regarding the longitudinal and lateral-directional derivatives, respectively.

4.1 Results on longitudinal plane

In this paragraph, the results related to CL, CD, and Cm vs the incidence α are illustrated.

The first noticeable result is (Figure 15) that the effect of the Reynolds number on the lift prediction is not significant so that the results on model 1 (full scale) and models 2 and 3 (1/4 scaled) are coincident; the introduction of the walls (model 4) produces modifications at increasing angles of attach (where the constraint of the walls is more effective) and, finally, with the modification of model 4 by introducing the k-ω transition (model 5), the value of CL given by CFD become coincident with the experimental results.

The CFD predictions of the total (induced plus friction) aerodynamic Drag according to the different models are summarized in Figure 16 in terms of Polar Curve. CD from models 1 and 2 are coincident (the Reynolds effect is insignificant for the small aircraft at hand) and CD is overestimated at high lift and strongly underestimated at low positive and negative CL (the effects of transitions are remarkable on the fuselage of the hydroplane, especially at small incidences); the introduction of the pylon and the walls (model 3 and 4) reduces the error and, again, with the modification of model 4 with the k-ω transition (model 5) the wind tunnel polar is exactly predicted by CFD, apart from small errors at high CL (about 1.2) and, with a larger error, at negative CL (where drag predicted by CFD is smaller than the experimental one due, probably, to the effects of flux separation around the hull redan). Table 5 shows a summary of CD_0 and K (the comparison of K is relevant to the intermediate range of CL).

The results on the pitching moment vs α are summarized in Figure 17. Again models 1 and 2 give the same results (Re is ineffective) and give predictions very far from the experiments because pylon and walls are missing. Model 3 and model 4 give accurate predictions in the significant range (0° - 12°) of incidence. The introduction of the k-ω transition in model 5 don't improve the agreement with experiments; probably the separation criterion adopted is not accurate as far as the fuselage at hand is concerned (the separation for an amphibious plane seems a complex problem of CFD analysis).

This paper is a pre-print version of:
Cipolla, V., Frediani, A., Lonigro, E. *et al.* Aerodynamic design of a light amphibious PrandtlPlane: wind tunnel tests and CFD validation. *Aerotec. Missili Spaz.* **94,** 113–123 (2015). https://doi.org/10.1007/BF03404694

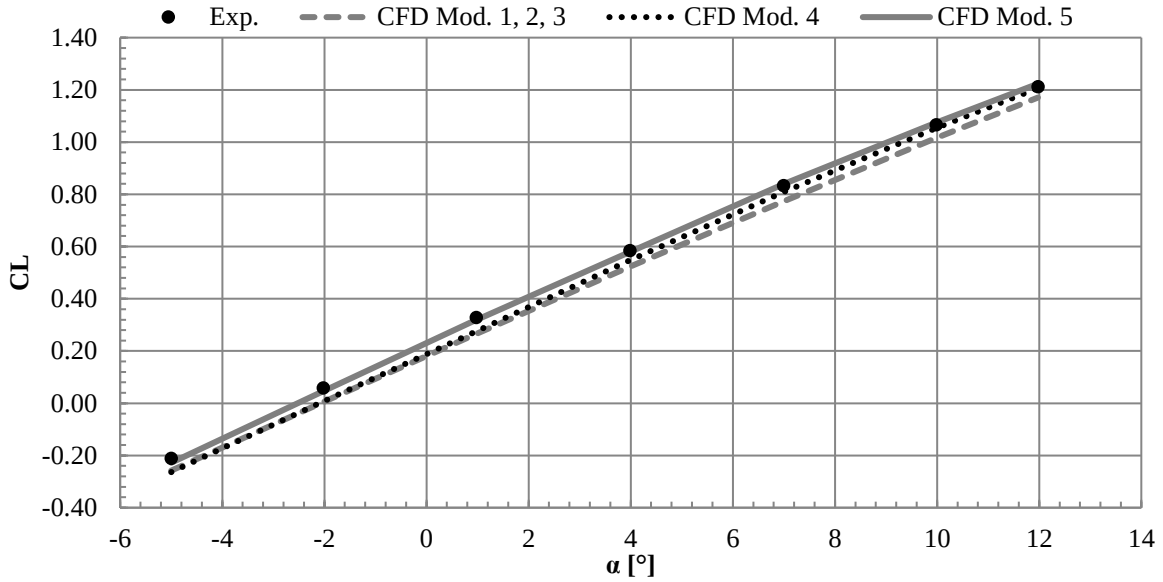

Fig. 13 Experimental and numerical CL vs α curves

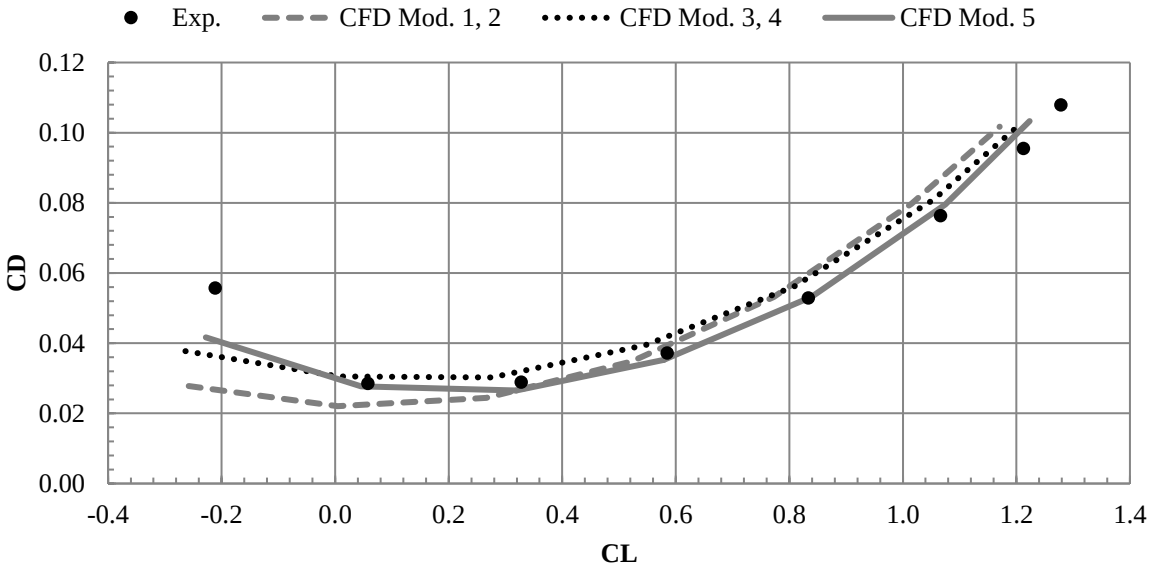

Fig. 14 Experimental and numerical polar curves.

This paper is a pre-print version of:
Cipolla, V., Frediani, A., Lonigro, E. *et al.* Aerodynamic design of a light amphibious PrandtlPlane: wind tunnel tests and CFD validation. *Aerotec. Missili Spaz.* **94,** 113–123 (2015). https://doi.org/10.1007/BF03404694

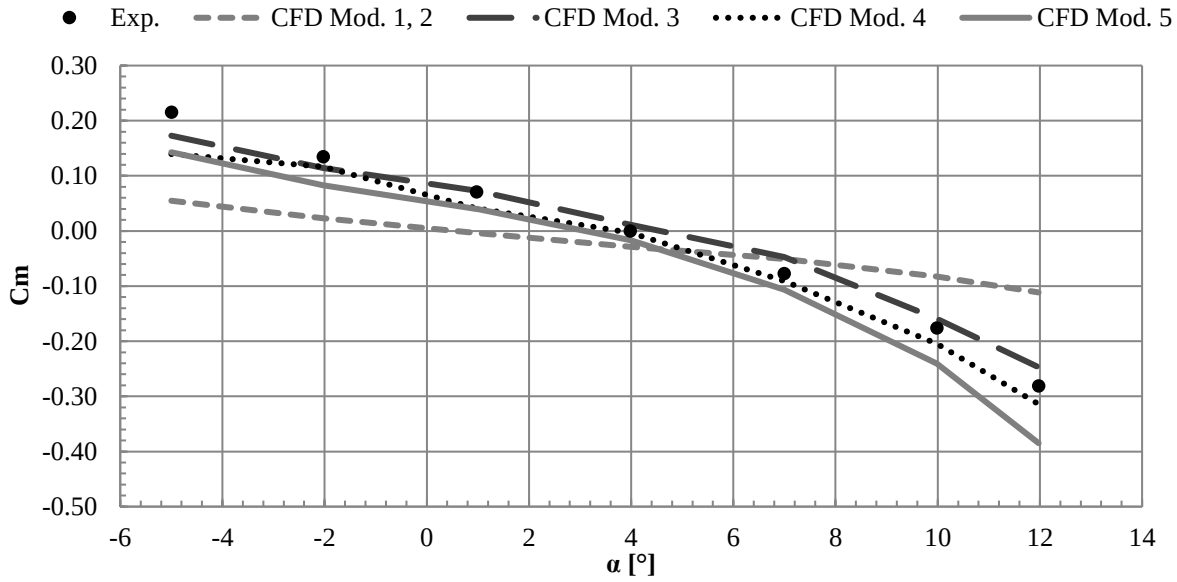

Fig. 15 Experimental and numerical Cm vs α curves

Table 4 Longitudinal coefficients variations in respect to experimental data

	Percentage variations CONTROLLARE DEFINIZIONE DI ERRORE %				Absolute variations????NON CHIARO	
α [°]	CL		CD		Cm	
	k-ε	k-ω	k-ε	k-ω	k-ε	k-ω
-5	24.7	7.7	-32.2	-25.2	-0.075	-0.072
-2	-89.1	-21.2	7.2	-2.9	-0.018	-0.052
1	-15.8	-2.6	4.6	-8.2	-0.029	-0.031
4	-6.5	-0.9	6.1	-5.2	-0.003	-0.017
7	-2.9	0.8	6.2	0.6	-0.014	-0.029
10	-1.2	0.8	6.0	4.2	-0.028	-0.064
12	-0.5	0.9	7.2	8.2	-0.033	-0.104

Table 5 Comparison between experimental and CFD drag polar parameters

	CD_0	K
EXP	0.030	0.0004
k-ε	0.032	0.0005
k-ω	0.030	0.0004 [6]

[6] Calculated by excluding the extreme values of CL

4.2 Results on lateral-directional plane

A CFD analysis on the lateral-directional plane has been conducted for α=1° and α=12° and β varying in the = 0° ÷ 10° (k-ω transition) and b=0° -12° (K-ε); the values obtained for lateral force (CY), rolling moment (Cl) and Yaw moment (Cn) coefficients are described in the following.

The CY vs β results are summarized in Figure 18; it appears that, for small β angles, the presence of the pylon and the walls has no effect and a small difference occurs for β > 10°; contrary to the other cases, the k-ω transition doesn't produce any improvement of accuracy.

The results on the CFD prediction of Rolling Moment (Cl) vs β are summarized in Figure 19 and compared with the experimental results. Models 1, 2 and 3 give the same results and are represented by a single curve, which is very far from the wind tunnel results. The introduction of the walls in the analysis (model 4) is fundamental for the prediction of a correct behavior of lift in the presence of yaw angles for this aircraft; the results with the k-ω transition are only partial but the effect doesn't appear so significant.

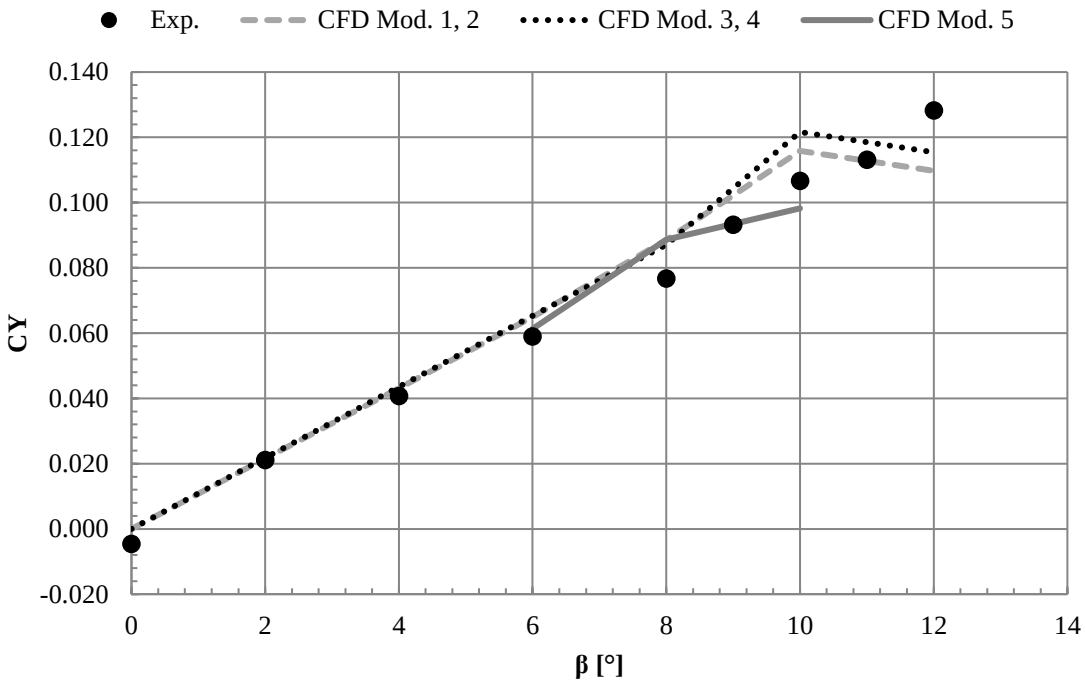

Fig. 16 Experimental and numerical CY-β curves at α=1°

This paper is a pre-print version of:
Cipolla, V., Frediani, A., Lonigro, E. *et al.* Aerodynamic design of a light amphibious PrandtlPlane: wind tunnel tests and CFD validation. *Aerotec. Missili Spaz.* **94,** 113–123 (2015). https://doi.org/10.1007/BF03404694

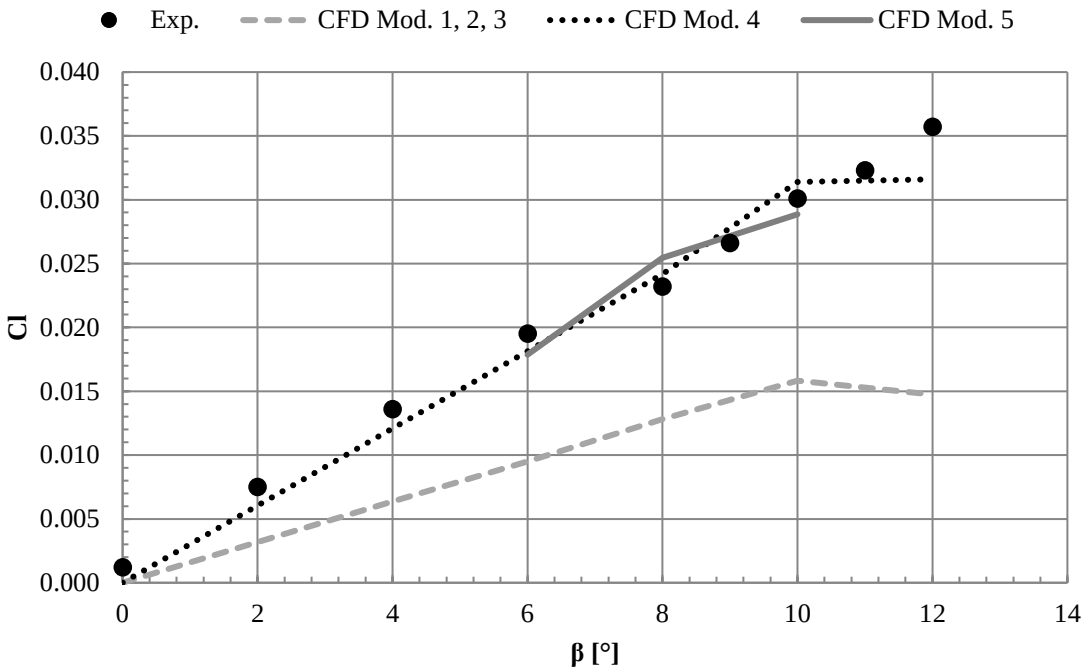

Fig. 17 Experimental and numerical Cl-β curves at α=1°

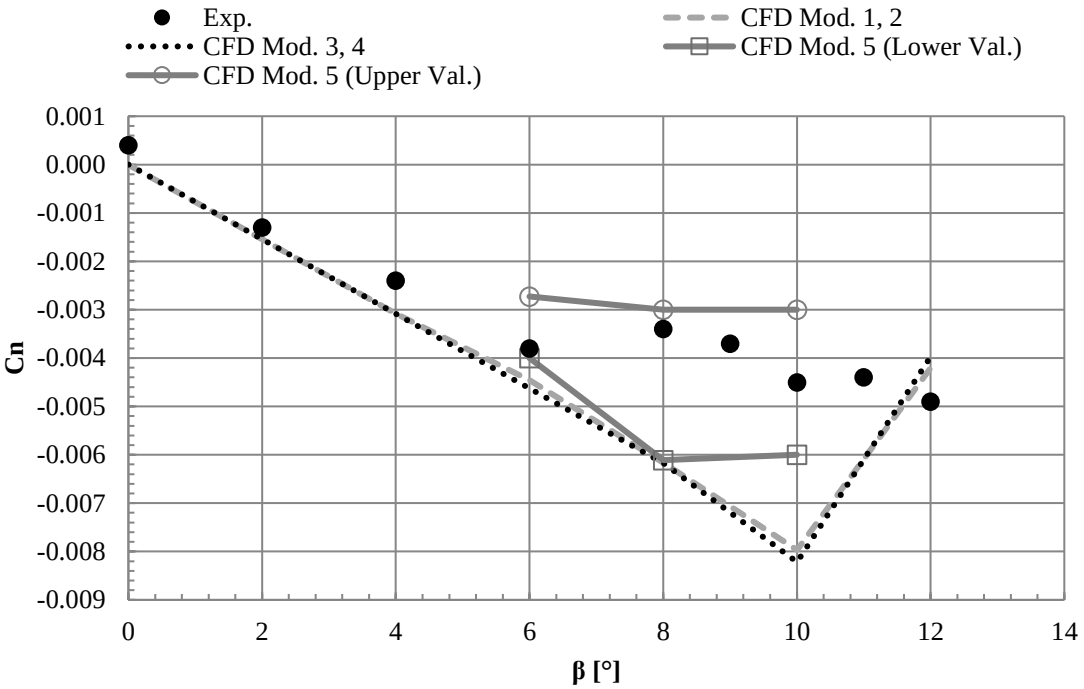

Fig. 18 Experimental and numerical Cn-β curves at α=1°

The particular behavior of Cn coefficient found in the wind tunnel cannot be replied with any geometrical configuration while using a k-ε turbulence model. Using instead a k-ω fixed transition solver a oscillating solution is obtained, and therefore the results have been divided between the maximum and minimum peaks.

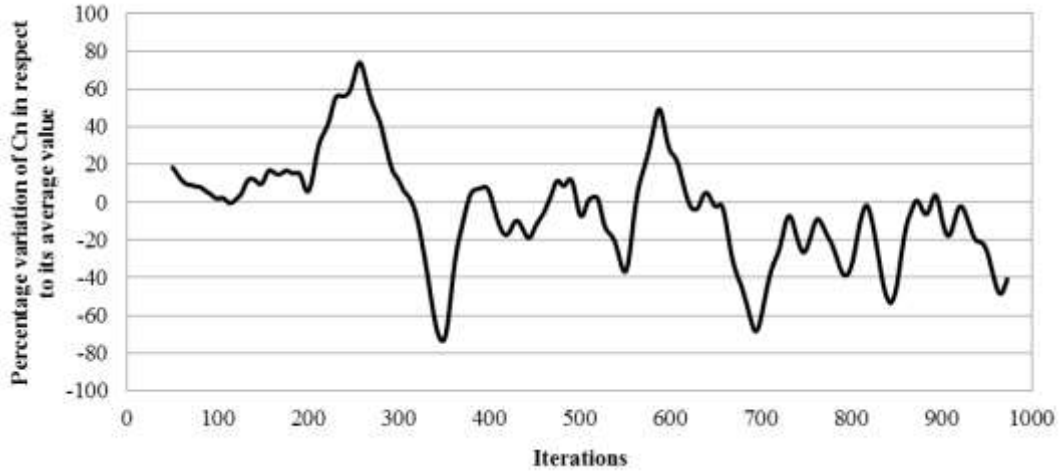

Fig. 19 Cn trend during the iteration for α=1°, β=10°

The cause of this behavior had been found in the tail zone by several visualizations along different horizontal planes.

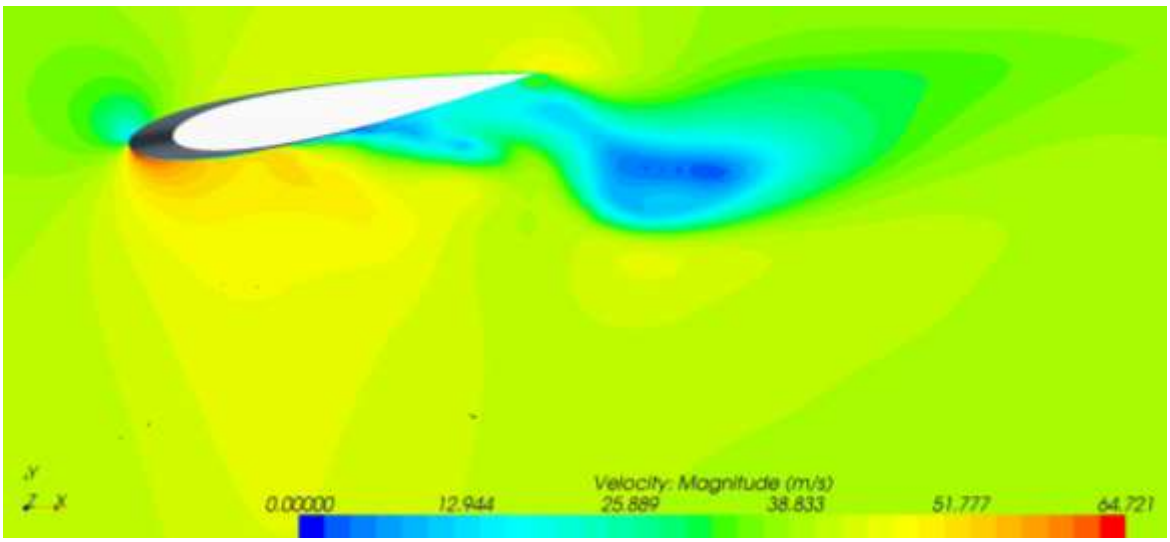

Fig. 20 Velocity magnitude in the tail zone, α=1°, β=10°

During the iteration, several vortexes (whose center is in the darkest blue zone) detach from the fin in the laminar region, generating the oscillating value of yaw previously seen. This kind of phenomenon is caused by the intersection of two suction peaks: the one generated by the tail and the one generated by the rear wing. In fact, for reasons related to the flight safety and mechanics the upper wing has been designed with a negative geometrical α angle, so its suction peak is

on the down side of the aerodynamic profile. When the aircraft is put in $\beta \neq 0°$ conditions another peak is added to the previous and so the flow has to face a strongly adverse pressure gradient obtaining finally a separation of the flux. This interference effect is higher moving closer to the rear wing, and the separation region increases, generating a conical-shaped separated flux.

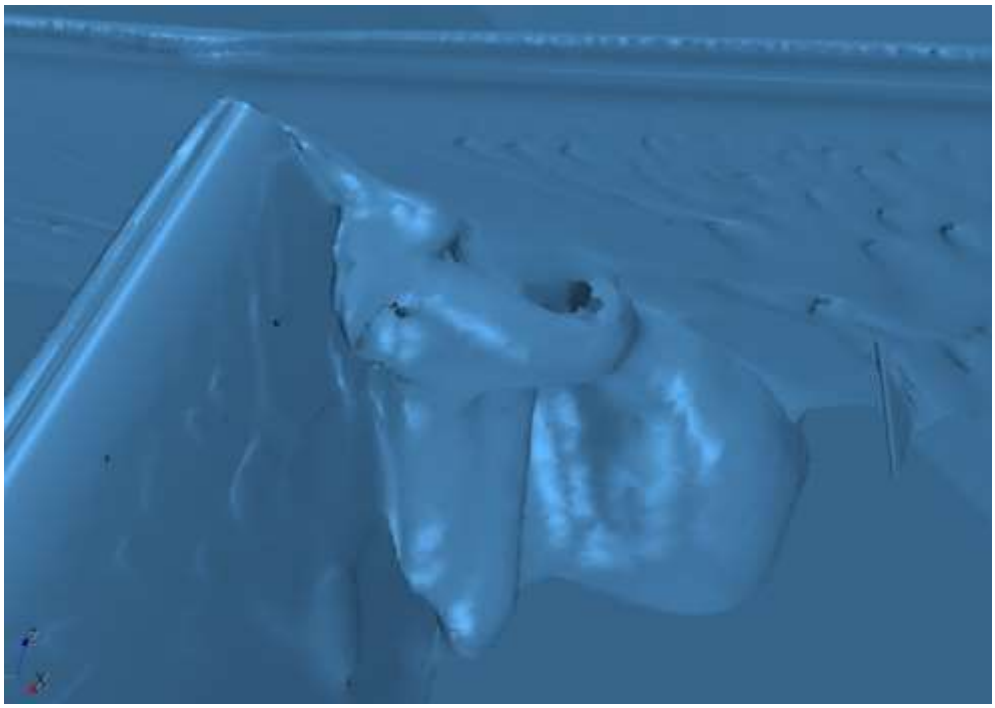

Fig. 21 Separation cone

Ascertained the prediction capacity of the k-ω solver for the lateral-directional coefficient, no further study with the k-ε model has been conducted, obtaining directly the following results.

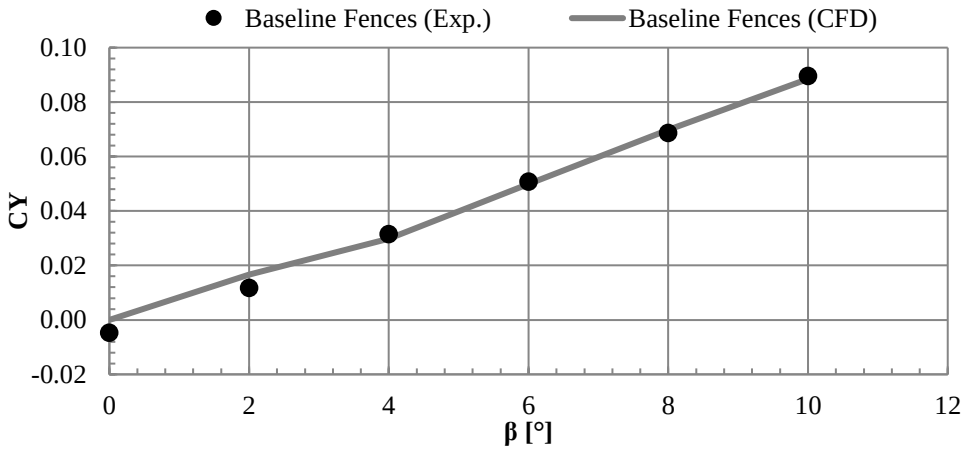

Fig. 22 Experimental and numerical CY-β curves at α=12°

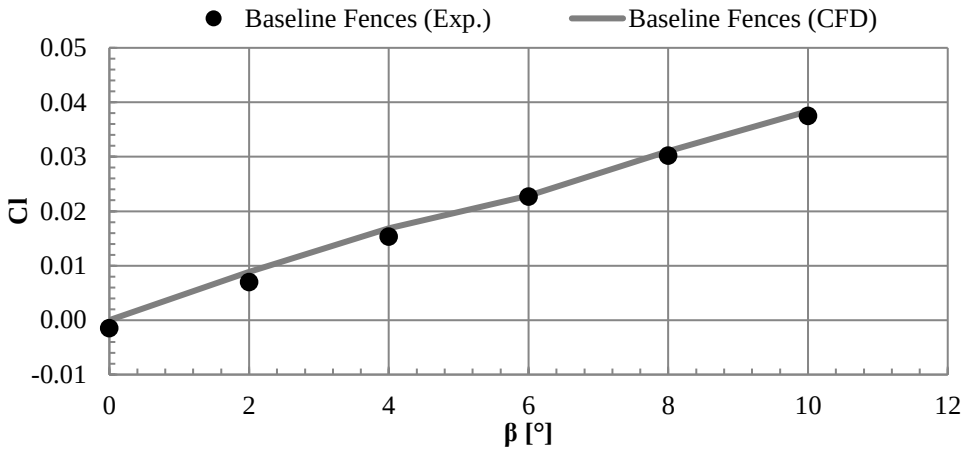

Fig. 23 Experimental and numerical Cl-β curves at α=12°

The results regarding the lateral force and the rolling moment reported have a good correspondence to the experimental ones, therefore they need no other discussion.

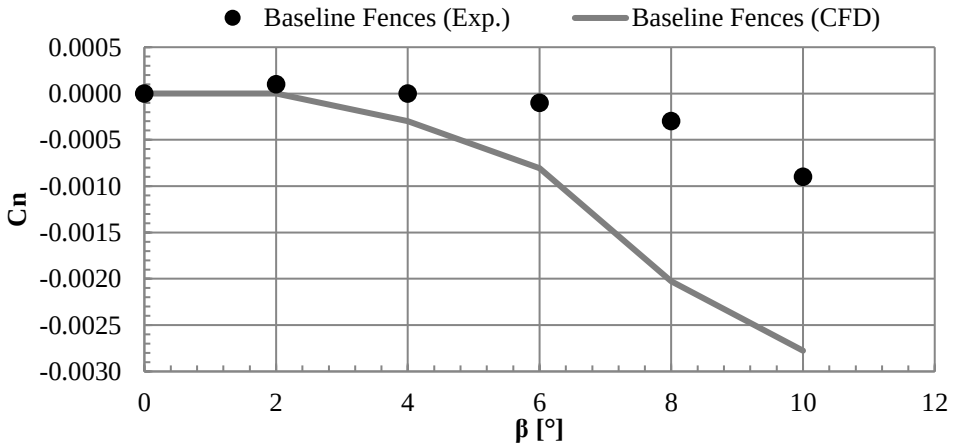

Fig. 24 Experimental and numerical Cn-β curves at α=12°

Visually, the CFD prediction seems to show a stable yaw behavior, it is though important to notice that, for α=12°, the coefficient is at least one order of magnitude smaller than the α=1° case and so is related to a very poor stabilizing moment. Hence, considering the not acceptable characteristics in the lateral directional plane, several solutions have been considered to improve the directional performance.

5. CFD ANALYSES FOR THE IMPROVEMENT OF DIRECTIONAL STABILITY

To improve the directional stability a variety of solutions have been discussed, finally deciding upon a fences extension.

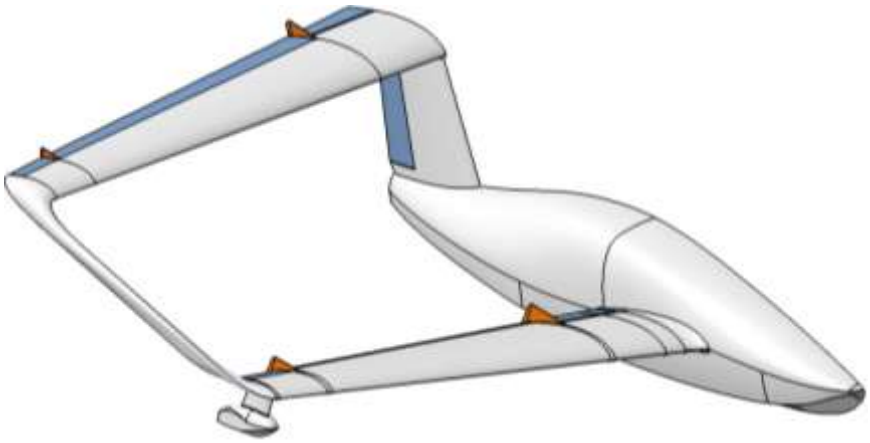

Fig. 25 Fences (orange colored)

The fences are aerodynamic surfaces previously studied to separate the fluxes on the different control surfaces (ailerons, flaps and elevators). However, their contribution to the stabilizing yaw moment is appreciable, so an improvement of their surfaces, in this case of the ones next to the elevators of the rear wing, has been realized and tested with the use of CFD simulations.

5.1 Modification of the fences

The extension of the aerodynamic surface is based on a series of tests previously conducted in the wind tunnel, where ad additional part was attached to the tail, prolonging the rudder, and obtaining in this way a satisfactory augmentation of stability.

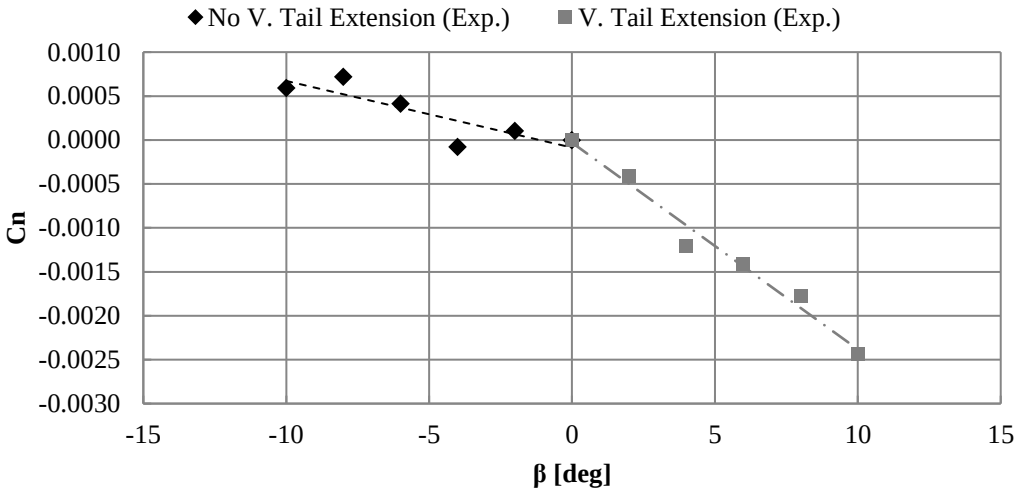

Fig. 26 Effect of vertical tail extension on directional stability

Taken as reference the value of additional surface used in the test, and dividing this number by two, the ulterior surface to be applied to the single fence was obtained. Three different solutions for this problem were studied and showed in Fig. 27.

The three modifications all have the same additional surface, but the most efficient is the A. That is because this configuration, particularly studied to correct the stability issue at high incidence, is the only one that works in a region of "clean" flow, which is not part of the dense wake that detaches from the fuselage, that acts as a bluff body for high incidences. The prolongation of the fence happens with the stretch along its direction of the relative trailing edge, until the fence surface has reached the desired value. Defined then the new fence geometry, its surface mesh has been generated, obtaining then a new general configuration, volume mesh and a set of new simulation, launched with a k-ω solver for $\alpha = -1°$ and $12°$ with respectively $\beta = 6° \div 10°$ and $\beta = 0° \div 10°$ angles.

The results given by the CFD are subsequently reported.

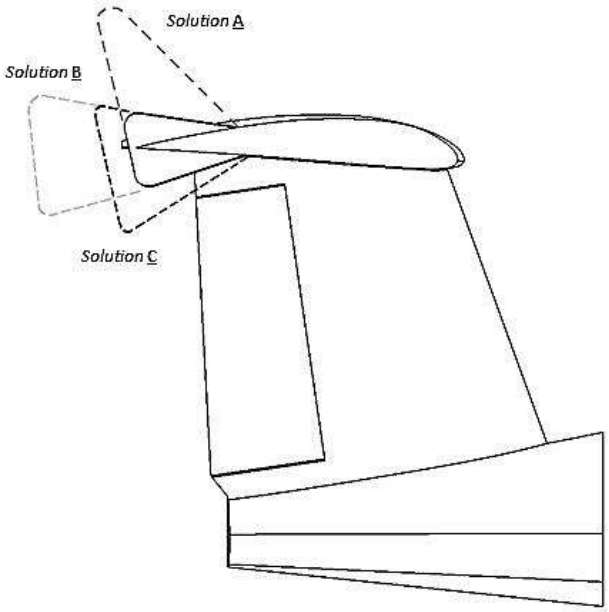

Fig. 27 Fences modification study

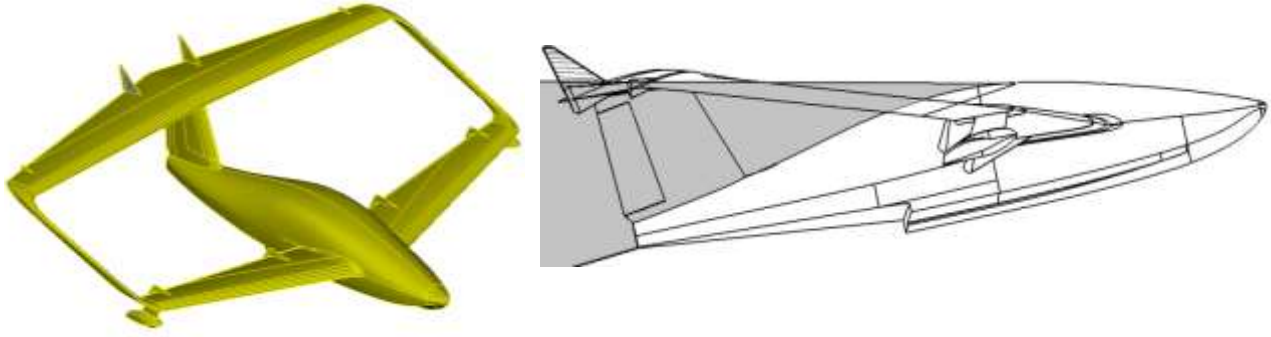

Fig. 28 Final configuration of IDINTOS (left) and modified fences position in respect to the fuselage wake (right)

5.2 Results for α=1°

Using the previously exposed k-ω CFD settings a test campaign has been conducted on the yaw moment for the α=1° condition and for β angles between 6° and 10°. While a slight improvement of rigidity is showed for CY and Cl in Fig. 29, Cn coefficient exhibits still a oscillating behavior, but of a minor intensity. Besides, a global linearity condition is reached, both with minimum and maximum values, in those zones which had before huge stability issues, that is the neighborhood of β=8°.

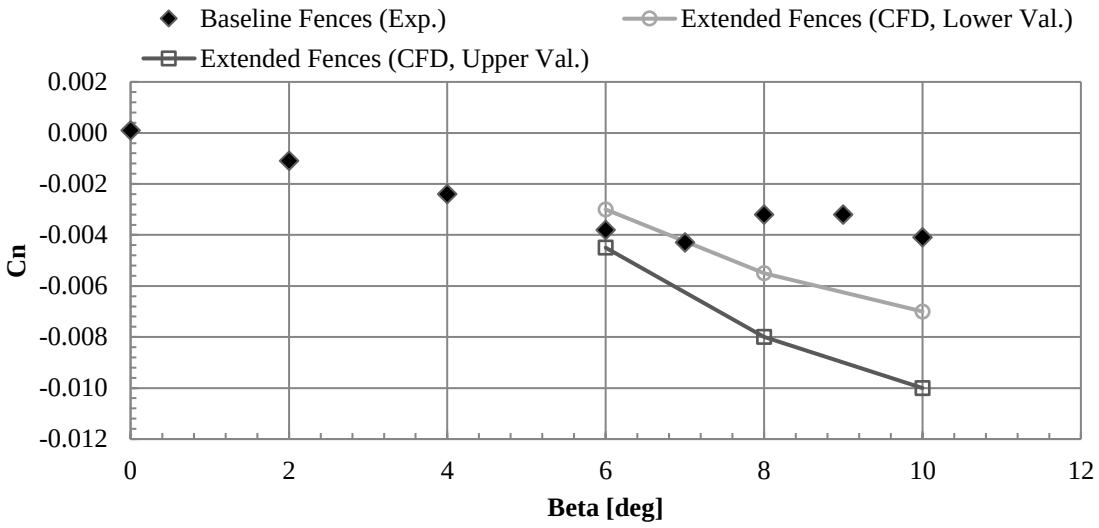

Fig. 29 Cn-β curves with extended fences at α=1°

5.3 Results for α=12°

As before, the fences have been tested also for high incidences and for β angles between 0° and 10°. The result, as expected, is a general improvement of directional stability, for all the tested β, augmenting by an order of magnitude (and then reaching the order of the values recorded for the α=1° case) the Cn coefficient. This kind of trend is satisfactory, so it can be assumed that the rigidity issue, both for low and high α incidences, has been fixed.

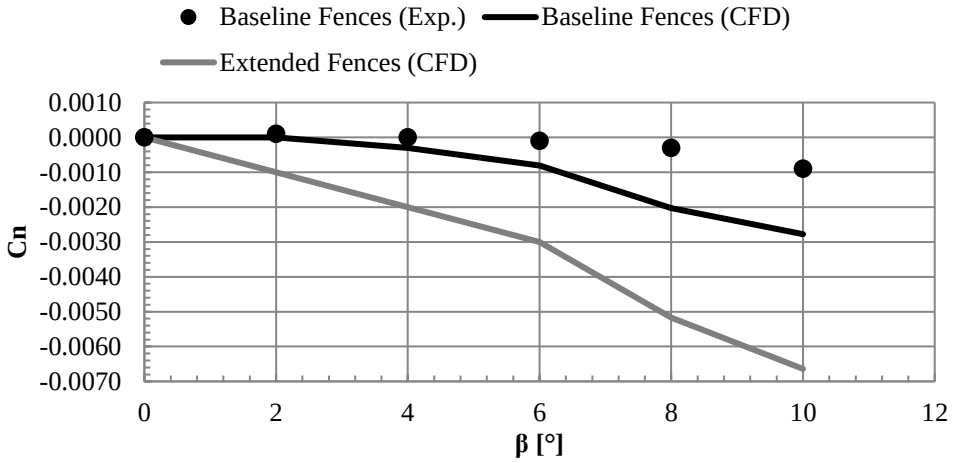

Fig. 30 Cn-β curves with extended fences at α=12°

6. CONCLUSIONS

The design of a new light amphibious PrandtlPlane was supported by towing tank tests, wind tunnel tests and flight tests on scaled models and, also by a huge amount of CFD analyses both regarding the aircraft design and, also, regarding the simulations of the tests themselves. One example is the case of wind tunnel tests and the relevant CFD results, the main subject of the present paper.

The CFD campaign has demonstrated that the CFD analysis could become an accurate and robust instrument for the prediction of aerodynamic performances of aircraft when the parameters governing the CFD results are properly settled, especially in the case of a complex configurations (a boxwing, a floating fuselage, two wingtip auxiliary floats, complex system of flaps on both wings, etc.). But, on the other side, some conditions exist in which the wind tunnel tests reveal that the aircraft needs more and more attention from the numerical viewpoint. All these conditions pertain to the non-linear range of Aerodynamic and regard both longitudinal and lateral derivatives. Different models, described in the paper, have been introduced, characterized by an increasing refinement to simulate closer and closer the test conditions into the wind tunnel; the final refinement regards a constitutive aspect in order to include a more suitable model (k-ω fixed transition solver was introduced) with an evident improvement of accuracy for the characteristics related to the lift and also for drag and pitch moment derivatives.

The CFD results has been compared with those from the experimental tests conducted on the same model; the wind tunnel walls and the mounting pylon have significant effects on the results and they have to be always included in the CFD model, especially in the case of large pitch or/and yaw angles.

The k-ω solver provides better solutions than the k-ε in terms of accuracy of transition position and evaluation of non-viscous effects.

The CFD assessment of the yaw moment is critical from the numerical viewpoint; while increasing the iterations, an asymptotic oscillation of the yaw moment has been observed even though the CFD analyses are conducted in steady conditions: the extreme values of these oscillations correspond to the higher and the lower boundaries of the experimental results; it is hard to conclude something about this result and more studies will be necessary, including a repetition of the tests.

The most evident disadvantage registered in this work regarded the week lateral stability of the aircraft at hand, confirming what was registered before, during the wind tunnel tests; a modified model with a new larger rudder was tested with positive results. The CFD analysis confirm this result but shows also that many solutions are equivalent to this one; in particular, one simple arrangement has been chosen in which twin fenced s on the rear wind were modified; this solution has been also adopted in the ¼ flying model (Figure 33) and the flight test tests were positive.

Figure 33. Rear fences on the flying model.

7. REFERENCES

[1] Cipolla, V., Frediani, A., Oliviero, F., Rossi, R., Rizzo and Pinucci, M., "Ultralight amphibious PrandtlPlane: the final design," Aerotecnica Missili e Spazio (to be published).

[2] Frediani, A., Cipolla, V., Oliviero, F., Lucchesi, L., Lippi, T. and Luci, S., "A new ultralight amphibious PrandtlPlane: preliminary CFD design of the hull," Aerotecnica Missili e Spazio (to be published).

[3] Prandtl, L., "Induced drag of multiplanes," NACA Technical Note 182, 1924.

[4] Frediani, A., Cipolla, V. and Rizzo, E., "The PrandtlPlane Configuration: Overview on Possible Applications to Civil Aviation," in *Variational Analysis and Aerospace Engineering: Mathematical Challenges for Aerospace Design*, Buttazzo, G. & Frediani, A. *(Eds.)*, Springer US, 2012, pp. 179-210

[5] Cipolla, V., Di Ciò, F., Frediani, A., Oliviero, F., Roccaldo, M. and Rossi, R., "Ultralight Amphibious PrandtlPlane: Towing Tank Tests on a Scaled Model", *AIDAA XXII Congress Proceedings on Disc* [CD-ROM], AIDAA, Naples, Italy, 2013.

This paper is a pre-print version of:
Cipolla, V., Frediani, A., Lonigro, E. *et al.* Aerodynamic design of a light amphibious PrandtlPlane: wind tunnel tests and CFD validation. *Aerotec. Missili Spaz.* **94,** 113–123 (2015). https://doi.org/10.1007/BF03404694

[6] Cipolla, V., Frediani, A., Oliviero, F. and Gibertini, G., "Ultralight Amphibious PrandtlPlane: Wind Tunnel Tests," *AIDAA XXII Congress Proceedings on Disc* [CD-ROM], AIDAA, Naples, Italy, 2013.

[7] Italian Regulation for Ultralight Aircraft: D.P.R. n.133, July 9th 2010.

[8] McMasters, J. H., Kroo, I., Bofah, K. K., Sullivan, J. P., Drela, M., "Advanced Configurations for Very Large Subsonic Transport Airplanes," NASA CR 198351, Oct. 1996.

[9] Frediani, A., Montanari, G. and Pappalardo, M., "Sul problema di Prandtl della minima resistenza indotta di un sistema portante," *XV AIDAA Congress Proceedings*, AIDAA, Turin, November 1999, p. 267-278 (in Italian).

[10] Maggiari, E., "Aerodynamic CFD analysis of the innovative amphibious aircraft of the IDINTOS project," M.Sc. Thesis, University of Pisa, Department of Civil and Industrial Engineering, Aerospace Section, 2013.

[11] Lonigro, E., "Analisi CFD di un anfibio ultraleggero PrandtlPlane: validazione attraverso dati sperimentali di galleria del vento," M.Sc. Thesis, University of Pisa, Department of Civil and Industrial Engineering, Aerospace Section, 2014 (in Italian).